

Structural Approach of Sialon Glasses: M–Si–Al–O–N

J. J. Videau,^a J. Etourneau,^a J. Rocherulle,^b P. Verdier^b and Y. Laurent^b

^aInstitut de Chimie de la Matière Condensée de Bordeaux-CNRS-UPR 9048, Château Brivazac, Avenue du Dr. A. Schweitzer, 33608 Pessac Cedex, France

^bLaboratoire des Verres et Céramiques, URA CNRS 1496, Université de Rennes I, Campus Beaulieu, Bâtiment 10, Avenue du Général Leclerc, 35042 Rennes Cedex, France

Abstract

Glass samples with the formular composition: $M^{II}_{0.37}Si_{0.53}Al_{0.10}O_{1.58-3x/2}N_x$ ($M^{II} = Mg, Ca$ or Ba) and $M^I_{0.46}Si_{0.46}Al_{0.08}O_{1.27-3x/2}N_x$ ($M^I = Li$) have been studied by infra-red absorption spectroscopy. The nitrogen-free alkaline-earth glass structure is built up with SiO_4 and AlO_4 linked units as in the metasilicate glasses. The M^{II} cations are network modifiers, except Mg, which participate in the formative network inducing a certain part of the A^{3+} cations in six-fold co-ordination which play the role of network modifiers. The lithium glass presents a silicate layer structure formed with $(Si_2O_5)^{2-}$ units and Al^{3+} ions in four and/or five-fold co-ordination; the Li^+ cations are located between the layers. The presence of nitrogen leads to very high cross-linkage of aluminosilicate chain or layer. The M^{II} cations are inserted into increasingly large sites (Mg- to Ba- glasses). The structural change could be correlated with the physical properties: the network rigidity increases from Ba- to Mg- glasses and with the amount of nitrogen, and the disorder was emphasized with an increasing amount of nitrogen, but especially from Mg- to Ba- glasses. These effects are less perceptible for the lithium glasses with a layer structure. © 1997 Elsevier Science Limited.

1 Introduction

The partial substitution of oxygen by nitrogen in anionic vitreous networks, especially in aluminosilicates, involves profound modifications in the physico-chemical properties of these materials.^{1–7} These changes, including hardness, transition temperatures, elastic moduli, brittleness and viscosity have their origin in the number, nature, and force of the bonds generated by the partial replacement

of oxygen by nitrogen. Partial structural studies have been previously reported.^{8–10} To describe the change of average chemical bonding and structural arrangement, information about the evolution of the infra-red spectra may be useful, on the one hand, as a function of the nature of cations and, on the other hand, as a function of the nitrogen content. The structural change will correlate with the physical properties.

2 Experiment

The series of vitreous compositions in the Mg–Si–Al–O–N, Ca–Si–Al–O–N, Ba–Si–Al–O–N and Li–Si–Al–O–N systems were prepared as described in Refs 1, 3, 5 and 7 respectively.

The systems studied were chosen corresponding to $M^{II}_{0.37}Si_{0.53}Al_{0.10}O_{1.58-3x/2}N_x$, for $M^{II} = Mg, Ca$ or Ba , and $M^I_{0.46}Si_{0.46}Al_{0.08}O_{1.27-3x/2}N_x$ for $M^I = Li$. The nitrogen content (x) and the values of the N/(N+O) percentage for each M cation are reported in Table 1.

The vitreous compositions listed in Table 1 were studied between 200 and 1300 cm^{-1} using a Perkin Elmer 983 spectrophotometer. Starting from a suspension in nujol, samples as thin film were inserted between the two faces of two Csl monocrystal windows.

The compactness $\chi = \frac{A/C \cdot \rho_{exp}}{M}$ (A = the number of anions, C = the number of cations and M = the molar mass) values are derived from the density measurements (ρ_{exp}), determined using the hydrostatic pressure concept by immersing the samples in the CCl_4 . The uncertainty of the measurements is estimated to be $\pm 0.01 g cm^{-3}$.

The measurements of the microhardness (Hv) have been made in the Vickers scale of hardness with a Leitz apparatus. The pyramidal stamp is

Table 1. Composition and nitrogen percentage of the $M^{II}_{0.37}Si_{0.53}Al_{0.10}O_{1.58-3x/2N_x}$ ($M^{II} = Mg, Ca$ or Ba) and $M^I_{0.46}Si_{0.46}Al_{0.08}O_{1.27-3x/2N_x}$ ($M^I = Li$) studied glass samples

	M^{II}		M^I	
	x	$N/(N+O)$ (%)	x	$N/(N+O)$ (%)
M_1	0	0	0	0
M_2	0.033	2.11	0.027	2.00
M_3	0.066	4.27	0.054	4.11
M_4	0.100	6.53	0.080	6.28

obtained with the weight of 200 g after 20 s on the polished surface of the glass sample. The accuracy is $\pm 10 \text{ daNmm}^{-2}$.

The thermal expansion (α) measurements have been determined on small bars (10–20 mm of length) with ADAMEL DI 24–1600°C apparatus. The heating rate was 6°Cmn^{-1} in the 20–400°C range. The uncertainty of the measurements is estimated to be $0.25 \cdot 10^{-6} \text{ }^\circ\text{C}^{-1}$.

Glass transition (T_g), crystallization (T_c) and melting (T_f) temperatures have been accurately determined (deviation $< 5^\circ\text{C}$) with the assistance of a DTA TG92 Setaram apparatus on glass powders in nitrogen atmosphere. The heating rate was 5°Cmn^{-1} . The glass forming ability is given according to Hruby's criterion: $C_H = \frac{T_c - T_g}{T_f - T_c}$.

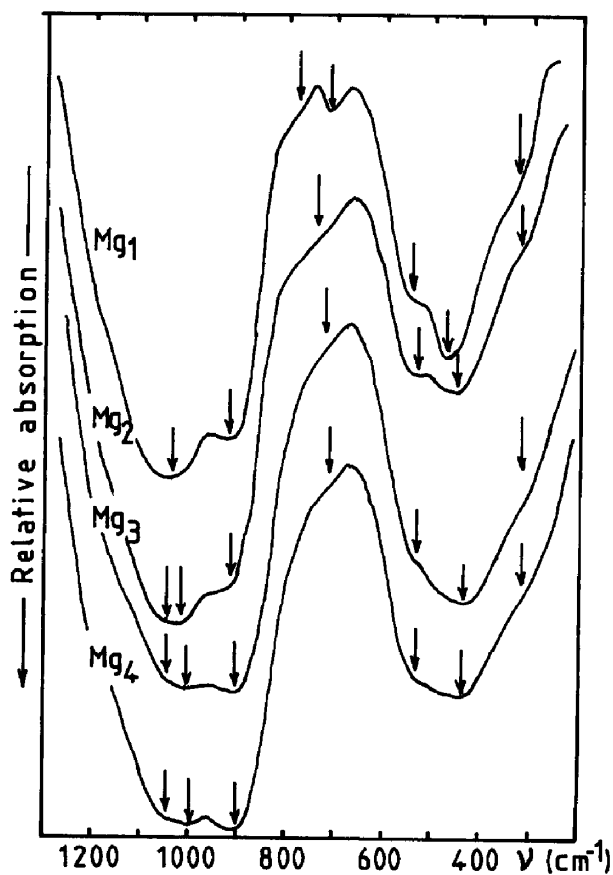


Fig. 1. IR absorption spectra of glass samples with the composition $Mg_{0.37}Si_{0.53}Al_{0.10}O_{1.58-3x/2}Nx$ (for x value see Table 1).

3 Infrared Absorption Study

The IR absorption spectra obtained for $M = Mg, Ca, Ba$ and Li are represented, respectively, in Figs 1–4.

3.1 Nitrogen-free glasses

These glasses correspond to the $x = 0$ composition in Table 1. IR spectra (Mg_1 in Fig. 1, Ca_1 in Fig. 2, Ba_1 in Fig. 3 and Li_1 in Fig. 4) present three absorption regions whose assignments are reported in Table 2.

The wide band located at high frequency is characteristic of asymmetrical stretching vibration modes of Si–O–Si bonds in the metasilicates.¹² The shift of the maximum of absorption of this band to the lower frequencies with the presence of double absorption in the $700\text{--}800 \text{ cm}^{-1}$ region seems to indicate the presence of aluminum in four-fold co-ordination in these glasses, in agreement with many authors.^{13,14} AlO_4 tetrahedra inserted into the silicate network form Si–O–Al bonds giving birth to $\nu(\text{Si–O–(Si, Al)})$ ($1000\text{--}1050 \text{ cm}^{-1}$; 780 cm^{-1}) and $\nu(\text{Al}_{IV}\text{–O})$ ($720\text{--}740 \text{ cm}^{-1}$) vibration modes. The band shift of the $\nu_{as}(\text{Si–O–(Si, Al)})$ vibrations towards the low frequencies (reverse effect for the shoulder of $\nu(\text{Si–O}^-)$ vibrations) with the size of M^{II} could be linked to an antagonistic bonding

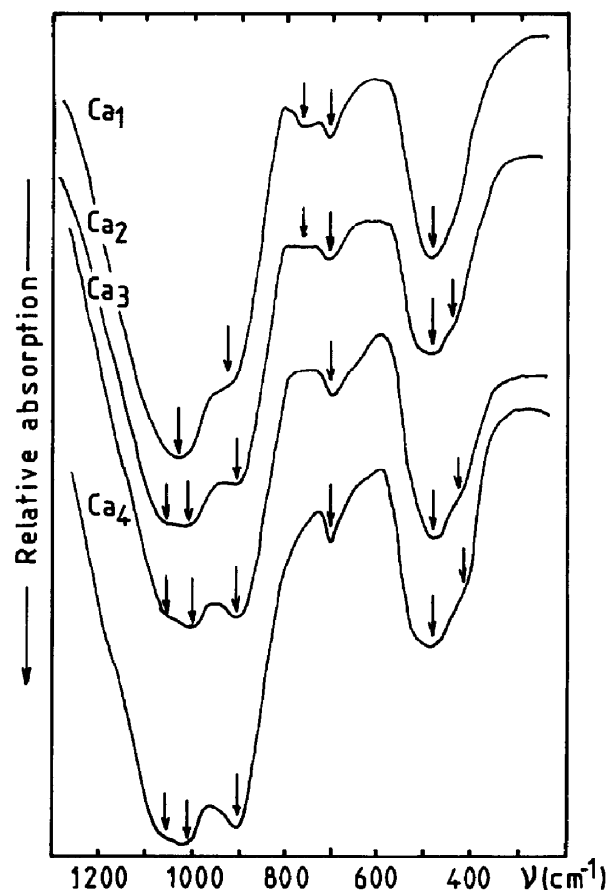


Fig. 2. IR absorption spectra of glass samples with the composition $Ca_{0.37}Si_{0.53}Al_{0.10}O_{1.58-3x/2}Nx$ (for x value see Table 1).

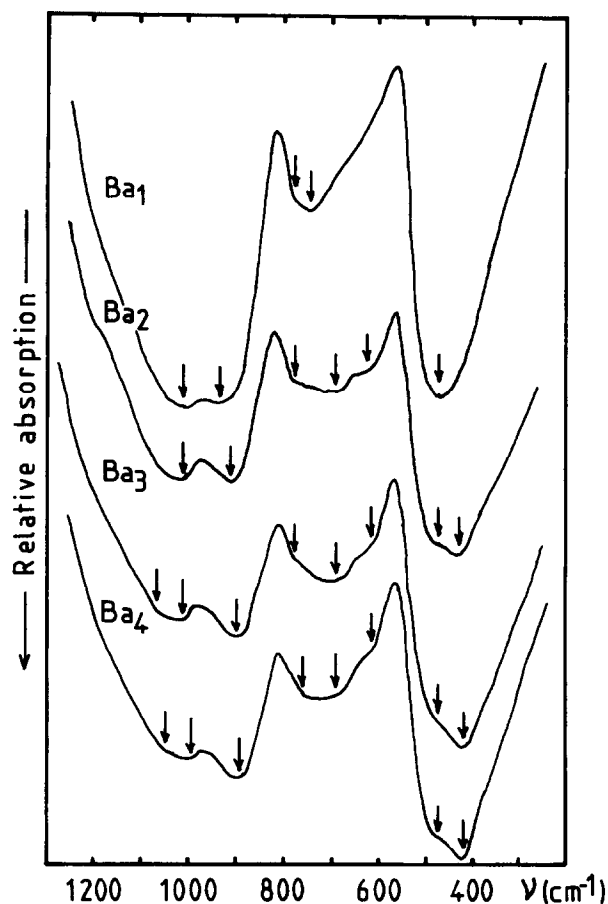


Fig. 3. IR absorption spectra of glass samples with the composition $Ba_{0.37}Si_{0.53}Al_{0.10}O_{1.58-3x/2}N_x$ (for x value see Table 1).

effect. The decrease of the electronegativity of the M^{II} causes a strengthening of the Si-O⁻ bond (ν (Si-O⁻), 900–940 cm^{-1}) and thus leads to a weakening of the Si-O-(Si, Al) bridging bond. This effect has already been observed in aluminosilicate glasses containing alkalines and alkaline earths.¹⁴

The broad band located at low frequencies (~ 500 cm^{-1}) is characteristic of O-Si-O bond deformational vibration modes.¹² For spectrum Mg_1 (Fig. 1), the shoulders at 550 cm^{-1} and 350 cm^{-1} , absent on the Ca_1 and Ba_1 spectra, are probably due to $\nu(Mg_{IV}-O)$ vibrations of MgO_4

Table 2. Positions and assignments of the absorption bands of the nitrogen-free glasses (s: shoulder, S: strong, m: medium, t: thin)

Mg_1	Ca_1	Ba_1	Li_1	Assignment
1100 sm	1100 sm	1100 s	—	ν_{as} Si-O-Si
1050 S	1030 S	1000 S	1040 S	ν_{as} Si-O-(Si, Al)
920 sS	930 sS	940 S	920 sS	ν Si-O-
780 st	780 t	780 sm	780 st	ν_S Si-O-(Si, Al)
720 t	720 t	740 m	740 m	ν $Al_{IV}-O$
			600 sm	ν $(Si_2O_5)^{2-}$
550 sS				ν $Mg_{IV}-O$
				ν $Al_{VI}-O$
480 S	500 S	480 S	450 S	δ O-Si-O
				ν $Li_{IV}-O$
350 st				ν $Mg_{IV}-O$

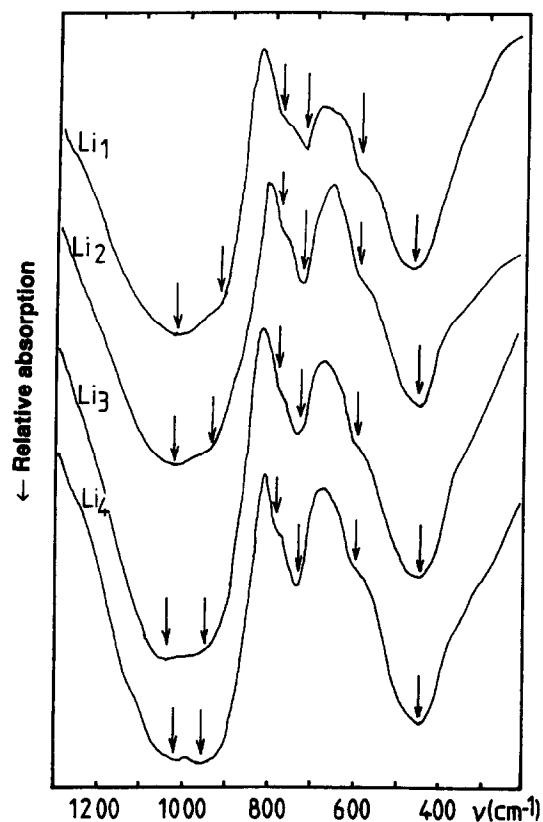


Fig. 4. IR absorption spectra of glass samples with the composition $Li_{0.46}Si_{0.46}Al_{0.08}O_{1.27-3x/2}N_x$ (for x value see Table 1).

tetrahedra as in vitreous¹³ or crystallized¹⁵ magnesium silicates. However, it is possible that the vibrations of AlO_6 are superimposed on those of the $\nu(Mg_{IV}-O)$ for 550 cm^{-1} . For Li_1 (Fig. 1), the shoulder located around 600 cm^{-1} could be assigned either to the Al atoms in six-fold coordination or, more probably, to the vibration mode of $(Si_2O_5)^{2-}$ units as in the silicate layers.¹⁶ The comparison of the spectrum Li_1 with those of obtained by TARTE¹³ for 6Li_2Si_2O_5 and 7Li_2Si_2O_5 glasses have allowed to explain that the strong absorption at the low frequencies may be due to the overlap of the LiO_4 tetradron and $\delta(O-Si-O)$ vibrational modes.

3.2 Oxynitride glasses

Generally speaking, an increase of the nitrogen content leads to the broadening of the band in the 800–1000 cm^{-1} absorption range with, simultaneously, an occurrence of two maxima at around 1050 and 1000 cm^{-1} for M_2 to M_4 (except for Li) and an increase of the intensity and a shift towards the low frequencies of the absorption band attributed to Si-O⁻ (M^{2+}) bond vibrations for M_1 . All of these modifications are due to the insertion of nitrogen into the silicate formative network with formation of the Si-N bonds which involves the weakening of neighbouring Si-O-(Si, Al) bonds with the appearance of $\nu(Si-N)$: around 1050 cm^{-1} , $\nu(N-Si-O \cdots (Si))$: between 970 and 1000 cm^{-1} ,

$\nu(\text{Si-N-Si})$: between 850 and 950 cm^{-1} vibration modes¹⁷ and/or $\nu(\text{Si-N})$ vibrations: around 950 cm^{-1} , in $(\text{N}_3\text{Si})\text{-O-(SiN}_3)$ molecular entities.¹⁸ The corresponding vibrations would become overlapped on those of the $\text{Si-O-(M}^{2+})$ non-bridging bond vibrations.

At the same time, in the 650–800 cm^{-1} absorption range, the characteristic band of the AlO_4 tetrahedra (730 cm^{-1}) disappears in Mg-glasses when nitrogen is introduced. This modification could be linked to the disappearance of the aluminium in a four-fold co-ordination, and to the partial replacement of oxygen atoms by nitrogen atoms around the aluminium in a four-fold coordination. Conversely, for the Ca-glasses, the band at 770 cm^{-1} slowly decreases up to $x = 0.1$. For the Ba-glasses, the absorption band greatly widens and its maximum (720 cm^{-1} for Ba_1) is displaced towards the lower frequencies with the increasing nitrogen content. In this case, the mixed environment around aluminium leads to the appearance of new vibration modes responsible for the widening of the absorption band. For the Li-glasses, the splitting at 740 and 780 cm^{-1} is always observed.

In the 400–600 cm^{-1} absorption range, the band characteristic in the oxide glasses of $\delta(\text{O-Si-O})$ deformational vibrations widen towards the lower frequencies (420 cm^{-1} for Mg-glasses), with the appearance of a shoulder at 400 cm^{-1} for Ca-glasses and a new maximum at 430 cm^{-1} for Ba-glasses which can be assigned to new deformational vibration modes of the O-Si-N bonds, in agreement with the assignments made for the absorption bands in the high frequency region. The simultaneous increase of the shoulder at 550 cm^{-1} due to the presence of MgO_4 entities ($\text{Mg}_2\text{-Mg}_4$) with the disappearance of the band at 730 cm^{-1} (AlO_4 entities), while the Mg/Si relationship remains constant, could be attributed to the change of aluminum from four-fold to probably six-fold coordination in the presence of nitrogen. For the Li-glasses, we note always the presence of the vibration mode of $(\text{Si}_2\text{O}_5)^{2-}$ units. The comparison of the Li_4 spectrum ($\text{Li/Si} = 1$) with the one of $\text{Li}_{0.54}\text{Si}_{0.39}\text{Al}_{0.07}\text{O}_{1.04}\text{N}_{0.07}$ glass composition ($\text{Li/Si} = 1.4$) allows one to observe an increase of the intensity of the band in the low frequencies (Fig. 5). This confirms that the lithium atoms are in four fold coordination.

4 Interpretation and Structure-Physical Property Correlation

The structural evolution of glasses as function of the nitrogen content closely depends on the structure of the oxide glasses, i.e. on the nature of M, according to the spectroscopic analysis.

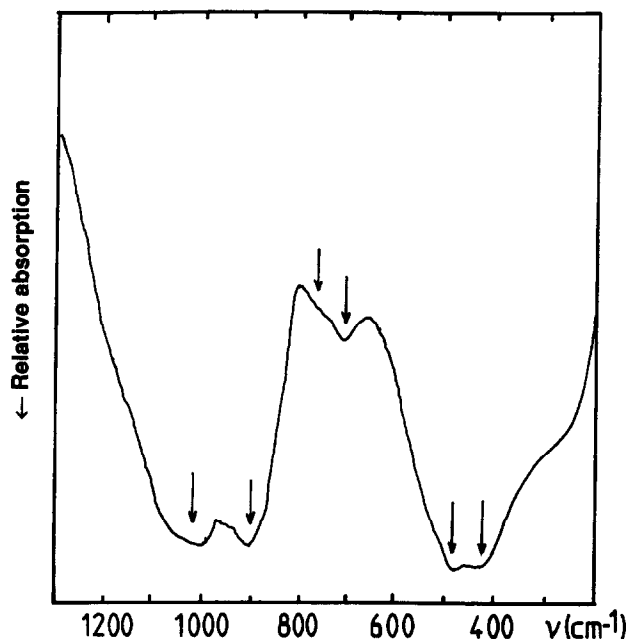


Fig. 5. IR absorption spectra of glass with the composition $\text{Li}_{0.54}\text{Si}_{0.39}\text{Al}_{0.07}\text{O}_{1.04}\text{N}_{0.07}$.

4.1 Nitrogen-free glasses

The M^{II}_1 glasses ($\text{O/Si} \approx 3$) probably have a meta-silicate structure close to MSiO_3 crystallized compounds.¹⁹ In the Mg_1 glass, the Mg^{2+} ions would be in four-fold coordination and located in the silicate formative network like a part of the Al^{3+} ions. The other Al^{3+} ions could be located in octahedral sites. All of the MgO_4 , AlO_4 and SiO_4 entities constitute the glass formative network with a few octacoordinated Al^{3+} ions playing the role of network modifier. This structure would present a high degree of compactness (Fig. 6) with a high degree of rigidity (Fig. 7) leading to the low thermal expansion value (Fig. 8) for Mg_1 glass. Furthermore, it gives rise to an oxide glass with high thermal stability illustrated by a high glass transition temperature (T_g) (Fig. 5). In the Ca_1 and Ba_1 glasses, the Al^{3+} ions in four-fold co-ordination are inserted in the silicate chains. The Ca^{2+} and Ba^{2+} ions play the role of glass network modifiers within large coordination polyhedra. These large sites, spreading out randomly in a relatively covalent formative network, induce a decreasing of compactness (χ_{Ca_1} and χ_{Ba_1}) and an increase in the vitrifying capacity (C_{HCa_1} and C_{HBa_1}), as shown in Figs 6 and 10, respectively.

The Li_1 glass with a composition close to $\text{Li}_2\text{Si}_2\text{O}_5$ probably has a layer structure built up with $(\text{Si}_2\text{O}_5)^{2-}$ entities. The Al^{3+} cations would be either in tetrahedral environment and located in the silicate formative network (but different with this one of silicium in agreement with the ROY's hypothesis (splitting of the 740 cm^{-1} band)¹⁴ or in pentahedral environment as observed by ^{27}Al NMR

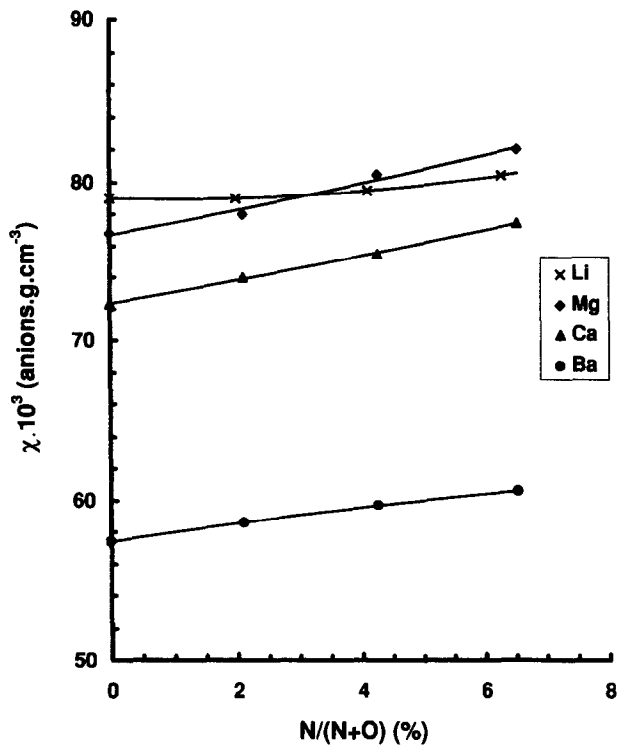


Fig. 6. Evolution of the compactness χ in relation to $N/(N+O)$ (%).

in the calcium aluminosilicate glasses.²⁰ The Li cations, in the four-fold coordination, are intercalated between these layers. Consequently, this glass structure is built up with AlO_4 and/or AlO_5 and SiO_4 units forming layers between which are inserted the lithium cations in four-fold coordination

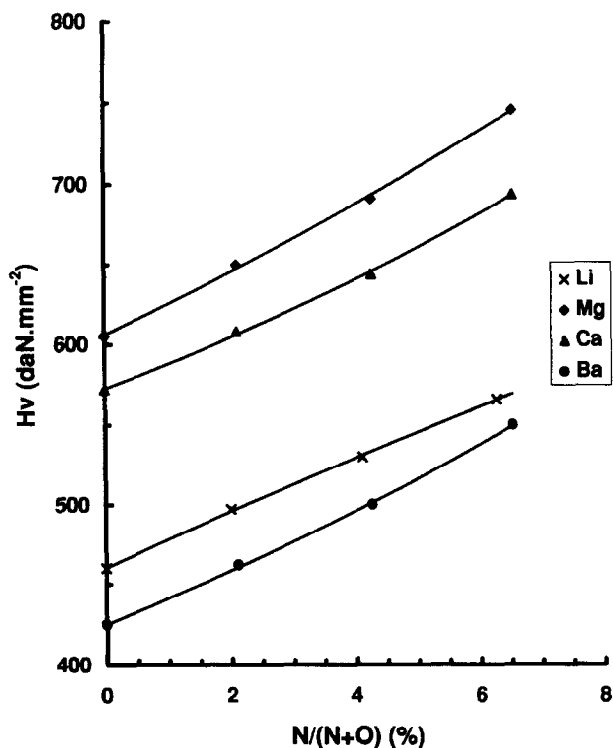


Fig. 7. Evolution of the Vickers microhardness H_v in relation to $N/(N+O)$ (%).

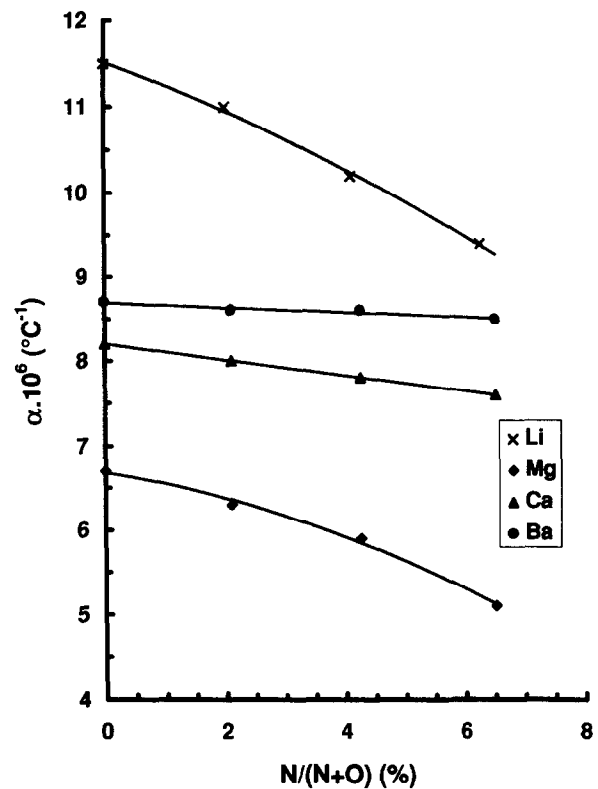


Fig. 8. Evolution of the thermal expansion $\alpha_{(20-400^{\circ}\text{C})}$ in relation to $N/(N+O)$ (%).

showing a better compactness than the one of Mg-glasses (Fig. 6) but a greater brittleness (Fig. 7) and a weaker thermal stability (Fig. 10). These two latter properties are probably linked to a soft cross-linkage between the layers with the Li^+ cations explaining the high thermal expansion value (Fig. 8).

4.2 Oxynitride glasses

The addition of nitrogen into these four families of glasses leads, in a general way, to the formation of Si-N bonds, thus tending to strengthen the silicate formative network.

In the case of Mg-glasses, the presence of nitrogen maintains the Mg^{2+} ions in the four-fold coordination, highly favoured in a nitrated silicate medium. On the contrary, in the presence of magnesium, all the Al^{3+} ions are six-fold coordinated as in the MgAlON spinel.²¹ The formation of Si-N bonds induces the formation of a majority of extra bridging bonds in relation to Si-O bonds leading to cross-linkage of the magnesium silicate chains which insert the Al^{3+} network modifying ions in octahedral site. The enhancement of the covalence of this network involves an improvement of all properties, as illustrated in Figs 6-10.

In Ca- and Ba-glasses, the Al^{3+} ions mainly remain in a four-fold coordination that contributes to the formative network. The nitrogen serves always as a cross-linking agent for aluminosilicate chain linkage. For these two types of glass,

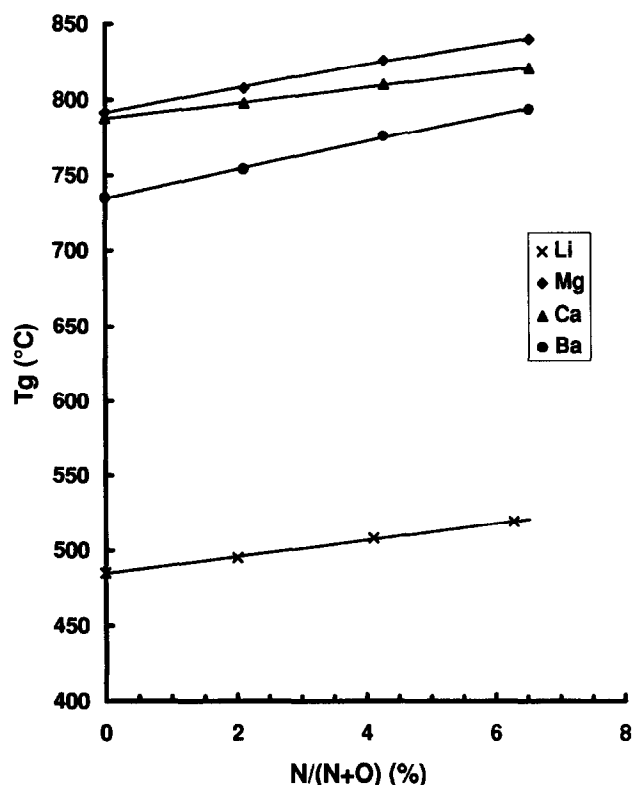


Fig. 9. Evolution of the glass transition temperature T_g in relation to $N/(N+O)$ (%).

cross-linkage seems to be greater than for Mg-glasses. As a matter of fact, the bands relative to the Si–N bonds, particularly for Ba₄ (890 and 420 cm^{-1}), are located at frequencies analogous to those found for highly nitrated crystallized or amorphous compounds, e.g. Si_3N_4 , $\text{Si}_2\text{N}_2\text{O}^{15}$ or

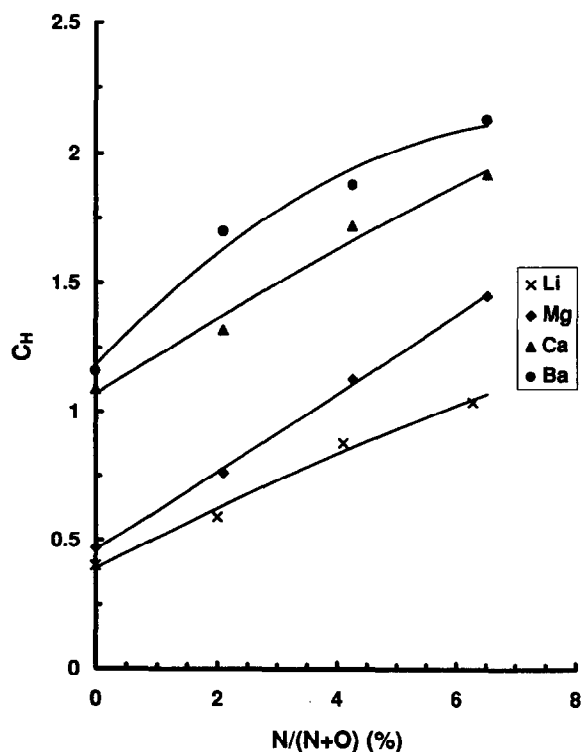


Fig. 10. Evolution of the Hruby factor C_H in relation to $N/(N+O)$ (%).

amorphous films with a composition $\text{Si}_5\text{N}_4\text{O}_4^{22}$ and the band, in the 800–600 cm^{-1} region (Ba-series), can be attributed to $\text{Al}_{IV}(\text{O}, \text{N})$ bond vibrations. In addition, the M^{2+} ions are surrounded by a large number of anions, with priority given to oxygen, then the number of bridging oxygens involved in the aluminosilicate formative network becomes small, leading to a greater concentration of nitrogen. The structural network of these glasses would be made up of a highly cross-linked nitrated aluminosilicate three-dimensional formative network randomly interrupted by many large cavities containing modifying cations, particularly barium. This interpretation can be correlated with the moderate evolution of the thermal expansion in relation to the nitrogen content (Fig. 8) in comparison with the Ca- or Li-glasses.

The introduction of the nitrogen in the Li-glasses leads to a similar evolution in most of the studied properties except for the compactness (Fig. 6) and the thermal expansion (Fig. 8). This means, probably, that the nitrogen substitution for oxygen is mainly located in the aluminosilicate layers which results in a greater covalency in the glass network (strong improvement of the thermal expansion) but a weaker bond between Li^+ cations and the glass forming network. This antagonistic bonding effect is liable for the weak evolution of the compactness with increasing nitrogen content, in contrast to the Mg-oxynitride glasses. This interpretation is in agreement with the enhancement of the electrical mobility of the Li^+ cations observed by REAU *et al.*²³

5 Conclusions

The study by IR absorption spectroscopy of the oxygen–nitrogen substitution in M aluminosilicate glasses shows that:

- i) in the Mg, Ca, Ba metasilicate glasses, the Si–N bonds are formed and, in the specific case of Mg-glasses, all the Al^{3+} ions migrate to octahedral sites. The presence of nitrogen leads to very high cross-linkage of the aluminosilicate chain forming a three-dimensional network into which the modifying ions (Ca^{2+} , Ba^{2+} or Al^{3+} for Mg-glasses) are inserted into increasingly larger sites (Mg- to Ba-glasses). The structural evolution of these glasses, depending on both M- size and nitrogen content, can be correlated with their physical properties. Thus it is shown that the rigidity of the network decreases from Mg- to Ba-glasses but, in contrast, the disorder increases with the nitrogen content;

ii) in the Li-silicate layer glasses, the formation of Si-N bonds strengthens the covalency of the aluminosilicate layers network but weakens the bond between Li⁺ cations and the glass forming network.

References

1. Verdier, P., Lemarchand, V. and Pastuszak, R., *Ann. Chim. Fr.*, 1982, **7**, 293.
2. Loehmann, R. E., *Journal Non Cryst. Solids*, 1980, **42**, 433.
3. Verdier, P., Pastuszak, R., Lemarchand, V. and Lang, J., *Rev. Chim. Min.*, 1981, **18**, 361.
4. Sakka, S., Kamiya, K. and Yoko, T., *Journal Non Cryst. Solids*, 1983, **56**, 147.
5. Verdier, P., Cohen, L., Mariotti, S. and Marchand, R., *Rev. Chim. Min.*, 1983, **20**, 1.
6. Tredway, W. K. and Risbud, S. H., *Journal Non Cryst. Solids*, 1983, **56**, 135.
7. Rocherullé, J., Guyader J., Verdier, P. and Laurent, Y., *Journal Mat. Sci.*, 1989, **24**, 4525.
8. Xu, X., Li, J. and Yao, L., *Journal Non-Cryst. Solids*, 1989, **112**, 80.
9. Videau, J. J., Etourneau, J., Garnier, C., Verdier, P. and Laurent, Y., *Mater. Sci. Eng.*, 1992, **B15**, 249.
10. Gervais, F., Blin, A., Garnier, C., Verdier, P. and Laurent, Y., *Journal Non-Cryst. Solids*, 1994, **176**, 69.
11. Hurby, A., *Czech. Journal Phys.*, 1972, **B32**, 1187.
12. Lazarev, A. N., *In Vibrational Spectra and Structure of Silicates*, Consultant Bureau, York and London, 1972, p. 106.
13. Tarte, P., *In Proc. Int. Conf. Phys. Non - Cryst. Solids*. Delf, The Netherlands, 1964, p. 549.
14. Roy, B. N., *Journal Am. Ceram. Soc.*, 1987, **70**(3), 183.
15. Gabelica-Robert, M. and Tarte, P., *Spectrochem. Acta*, 1979, **35 A**, 649.
16. Liebau, F., *Acta Cryst.*, 1961, **14**, 289.
17. Andrieckii, R. A., and Leont'ev, *Izv. Akad., Nauk. SSSR, Neorg. Mater.*, 1984, **20**(12), 2053.
18. Baraton, M. I., Labbe, J. C., Quintard, P. and Roult, G., *Mat. Res. Bull.*, 1985, **20**, 1239.
19. Lazarev, A. N., *In Vibrational Spectra and Structure of Silicates*, Consultant Bureau, New York and London, 1972, p. 140.
20. Coté, B., PhD thesis, University of Orléans, Orléans, France, 1993.
21. Granon, A., Goeuriot, P., L'Haridon, P., Guyader, J. and Laurent, Y., *Journal Eu. Ceram. Soc.*, 1994, **13**, 365.
22. Wong, J. and Angell, C. A., *In Glass Structure by Spectroscopy*. M. Dekker, Inc., New York and Basel, 1976, p. 547.
23. Réau, J. M., Kahnt, H., Rocherullé, J., Verdier, P. and Laurent, Y., *Journal Non-Cryst. Solids*, 1993, **155**, 185.